Materials Research Proceedings 28 (2023) 1583-1592 https://doi.org/10.21741/9781644902479-171

Influence of mesh in modelling of flow forming process

KRISHNAMURTHY Bhaskaran[1,a *], SHITIKOV Andrei A.[2,b], BLACKWELL Paul[3,c] and BYLYA Olga[1,d]

[1]AFRC, University of Strathclyde, 85 Inchinnan Drive, Inchinnan, Renfrew PA49LJ, UK

[2]QuantorForm LLC, 2nd Yuzhnoportovyy Proyezd, 16/2, Moscow 115088, Russia

[3]DMEM, University of Strathclyde, 75 Montrose Street, Glasgow G11XJ, UK

[a]bhaskaran.krishnamurthy@strath.ac.uk, [b]aa-shitikov@yandex.ru, [c]paul.blackwell@strath.ac.uk, [d]olga.bylya@strath.ac.uk

Keywords: Incremental Bulk Forming, Flow Forming, Meshing, Coarse Meshing

Abstract. Flow forming is an incremental bulk forming process used to produce tubular components from high-strength alloys. One of the features complicating its modelling is the small contact area of the workpiece with the tools. Taken along with cyclic non-monotonic loading from three rollers deforming the workpiece with complicated kinematics, this demands a very fine mesh and time step throughout the simulation. The typical approach of using a tetrahedral mesh with strain-based remeshing can introduce errors in the results due to the highly localized deformation and can also prolong the computation time. In the present study, in parallel to using tetrahedral mesh with remeshing, two different approaches of hexahedral mesh without any remeshing were also modelled for the workpiece, retaining all the other setup parameters, and the results compared. In both cases, local mesh adaptations were used to ensure a very fine mesh in the zone of contact with the rollers. Results from the simulations clearly showed that the key outputs such as stress state parameters (triaxiality and Lode stress parameters) and plastic strain values were very sensitive to the mesh and remeshing method used and careful consideration is required before employing the outputs for further analysis.

Introduction

Flow forming is an incremental bulk forming process employing two or three rollers that produce localized zones of deformation to manufacture near-net shape tubular components [1,2]. It is a flexible and effective method to produce parts from high-strength alloys with limited ductility at room temperature[3]. It is highly flexible as it affords the possibility of independent setting of up to seven process parameters (mandrel rotation speed, axial and radial displacement speeds of three independent rollers) as detailed in [4,5] and this enables different forming strategies depending on the material, component shape and machine capabilities. In addition, for large thickness reduction ratios of thick-walled workpieces with wall thinning of up to 80–90%, the process can be carried out in several passes [5,6].

However, the process is innately complex and deciding on a forming strategy or solving particular problems such as component fracture are not straight-forward. Finite-element (FE) modelling of the process can provide some much needed insight into the complicated process mechanics, but it is not without its fair share of complications, as detailed in the work of Bylya et al. [7]. One of the features of the flow forming process that complicates its modelling is the small contact area of the workpiece with the rollers. This circumstance imposes special requirements on the choice of the finite element mesh and the time step of the calculation. Consequently, the choice of mesh size and time step influences the output from the model considerably. The inaccuracy and errors resulting from the choice of mesh will impact further analysis such as fracture prediction

that uses the outputs from the simulation and therefore cannot be overlooked in the case of robust modelling required for industrial applications.

For finite deformations in bulk forming processes, typically, a tetrahedral mesh is employed in many commercial metal forming software and a strain-based remeshing algorithm is used to remesh the nodes and elements when the strain reaches a certain value, which can be set by the user. The remeshing is helpful to avoid distortion of meshes at very high strains and can be beneficial is most metal forming modelling for improving the accuracy of the model. However, in incremental bulk forming processes, such as flow forming, remeshing can introduce errors in the results due to highly localized deformation and can also prolong the computation time. The influence of mesh size and remeshing formulation has been reported in few earlier works [8,9]. The focus therein was limited to sensitivity analysis against a specific output value (von Mises stress) [9] or the differences between different formulation of the problem, i.e., Euler, Lagrangian or ALE[8]. In the present work, in parallel to the typical approach of using tetrahedral mesh with remeshing, alternative use of hexahedral mesh for the workpiece without any remeshing was also modelled, using the same Lagrangian formulation and retaining all the other setup parameters. The key output parameters from the models were analyzed and compared against actual experimental findings.

Experimental Data Used for Modelling

A relatively short process involving a single pass flow forming of Ti6Al4V tube of thickness 12 mm is taken for simulation and for comparison of the models. It was found experimentally with repeatability that Ti6Al4V preforms fractured before the roller reached a final depth of 9 mm (i.e., reduction of 3 mm (25%)). A finite-element simulation of the process will play a crucial role in understanding the reason behind the failure. Furthermore, owing to the short duration of the actual process prior to failure, i.e. 16 s, the process can be simulated completely using a full 3D elasto-plastic formulation and with fine mesh and time-step settings. A schematic of the process and process parameters used in the model setup are provided in Fig. 1 and the kinematics parameter used for the model setup are summarized in Table 1.

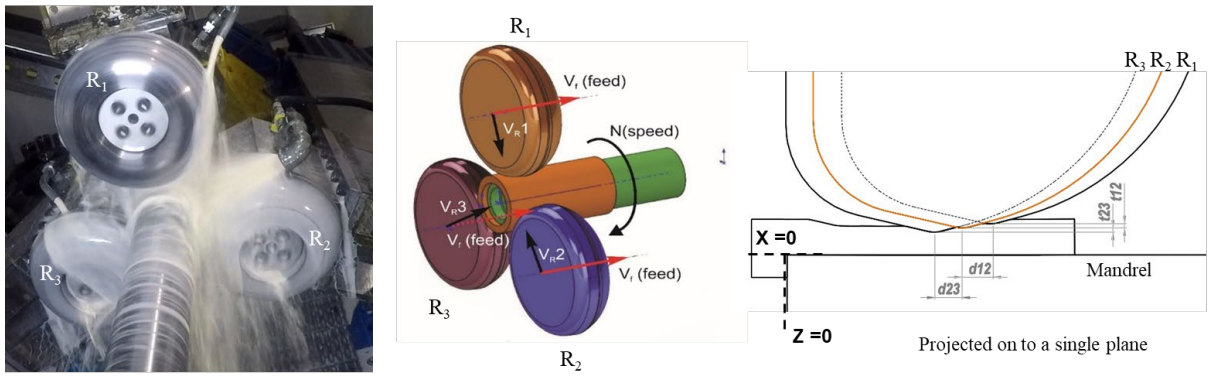

Fig. 1. Three-roller flow forming process - (a) capture of process carried out at AFRC, University of Strathclyde, (b) schematic of the process representing the main process parameters and (c) schematic showing the axial and radial positions of the three rollers when projected on to a single axial plane.

The rollers are located 120° apart in the circumferential direction as shown in Fig. 2 (a) and (b), with Roller 1 directly above the workpiece in what is designated as the vertical axis for the whole setup. The rollers are staggered both axially and radially. The total reduction is split between the rollers in such a way that Roller 1 has a bite of 1 mm, Roller 2 goes further deep with a radial

offset of 1 mm between Roller 1 and 2 (t_{12}) and Roller 3 goes even further deep with a radial offset of 1 mm between Roller 2 and 3 (t_{23}); in summary, the total bite of Roller 2 and Roller 3 are set to be 2 and 3 mm, respectively. In addition, Roller 2 trails behind Roller 1 by 4 mm (d_{12}), and Roller 3 trails behind Roller 2 by 4 mm (d_{23}) in the axial direction. When projected onto a single plane the roller offset will appear as shown in Fig. 2(c). A constant rotation speed of 150 RPM is prescribed to the mandrel and a tailstock is used to apply pressure across the face of the workpiece such that the workpiece rotates along with Mandrel without slipping. The rollers do not have their own spindle drives but rotate only due to the friction on contact with the workpiece.

Table 1. Summary of main process parameters used in experimental trials studied.

Speed, N [RPM]	Feed, V_f [mm/s]	Initial Thickness, t_0 [mm]	Final Thickness, t_f [mm]
150	1	12	9
Radial offset b/w Roller 1 and 2, t_{12} [mm]	Radial offset b/w Roller 2 and 3, t_{23} [mm]	Axial offset b/w Roller 1 and 2, d_{12} [mm]	Axial offset b/w Roller 2 and 3, d_{23} [mm]
1	1	4	4

Modelling Approach

To obtain a smooth deformation field when simulating the process, the roller must pass the contact zone in at least three time steps. The typical size of the contact spot according to experimental measurements for the case of the simulated process is approximately 9 × 16 mm, please refer to Fig. 2(a). With a workpiece rotation speed of 150 rpm and the external diameter of the part being 164 mm, the calculated time step should not exceed 4 ms. In order for at least 8–10 workpiece nodes to be in contact with the roller (blue dots in Figure 2a), the required size of the finite element mesh element should not exceed 2 mm; this is also necessary for the correct modelling of the plastic deformation gradient, and the resulting residual stresses, across the thickness of the workpiece (Fig. 2(b)). Furthermore, elastic deformation of the rest of the workpiece and secondary plastic deformation of the already deformed regions also play a crucial role, and therefore a relatively fine mesh is also required in regions that are in the vicinity of contact with rollers and also in already deformed regions.

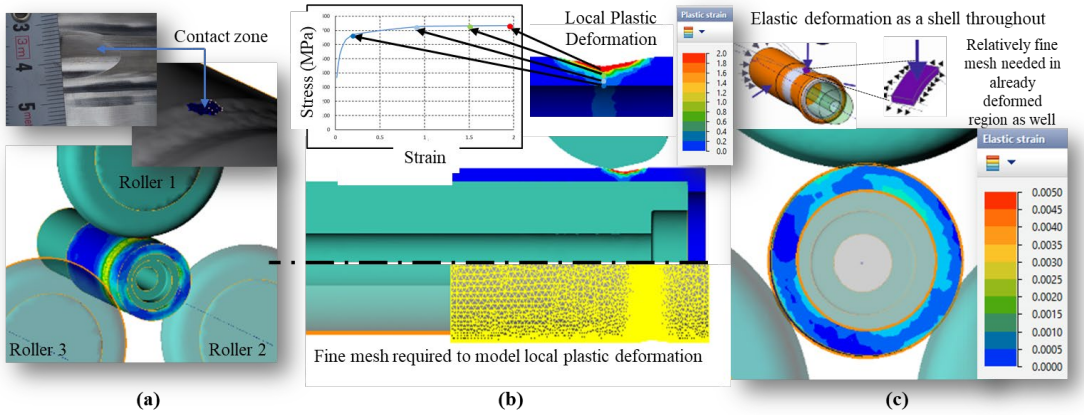

Fig. 2. Factors influencing the finite element mesh when modelling flow forming: a) small contact area between the workpiece and rollers (inset: measurement from experiment and that observed in FE simulation), b) local plastic deformation (showing the gradient of plastic strain along thickness), c) elastic deformation of workpiece as a shell throughout.

To analyze the influence of mesh settings, 3 different cases were simulated as shown in Fig. 3: Case I - default tetrahedral mesh with strain-based remeshing (Fig. 3 (b)); Case II – a coarse hexahedral mesh with less than 2 mm element size in the contact zone without remeshing through the process (Fig. 3 (c)); Case III - a finer hexahedral mesh with less than 1 mm element size in the whole deforming region of workpiece without remeshing through the process (Fig. 3 (d)). Only the first 16 s of the process leading to the fracture were simulated in each case. In Case I and II, a local mesh adaptation covering the expected contact zone with the three rollers through the process was used to refine the initial mesh to 1 mm and 2 mm, respectively. In regions outside the mesh adaptation, an average mesh sizes of 5-8 mm were used in both cases. In Case III, a fine mesh with average element size of 1 mm was used in the region covering the expected start of contact with rollers to the end of the workpiece as shown in Fig. 3 (d). The nose region in the rollers, which typically contact the workpiece, were also meshed fine as shown in Fig. 3 (a) to ensure proper contact area calculations.

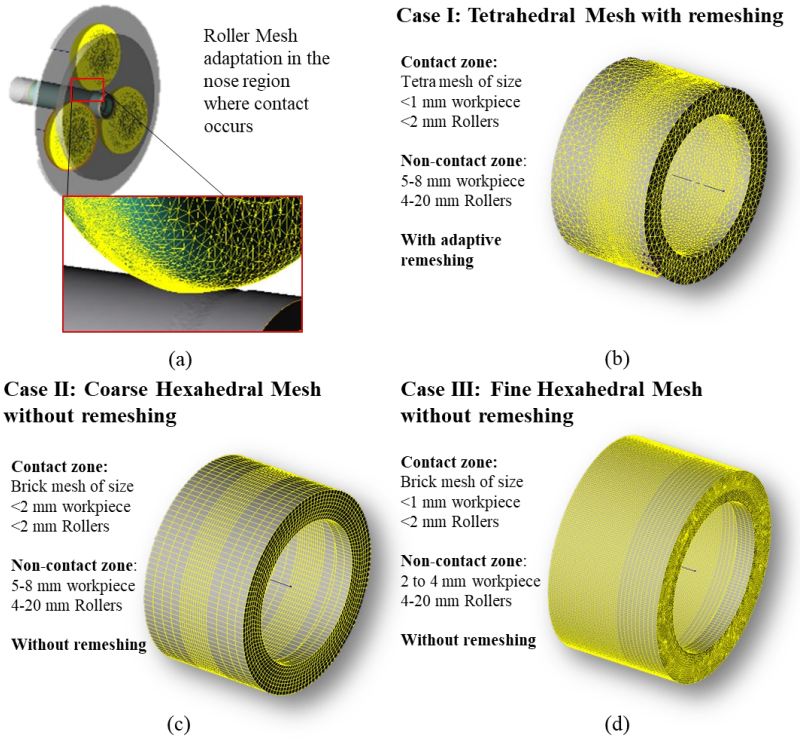

Fig. 3. Mesh settings used in the study – (a) Mesh adaptation used in the nose region for meshing of rollers to simulate accurate contact with workpiece; Workpiece mesh settings used in (b) Case I with tetragonal mesh and strain-based remeshing, (c) Case II with relatively coarse hexagonal mesh and without remeshing through process, and Case III with finer hexagonal mesh and without remeshing through process.

All the cases were simulated using commercial metal-forming software, QForm. The tool kinematics in the model setup were maintained as close to the real process as possible and were the same in all 3 cases. A full 3D elasto-plastic model with isotropic hardening material model obtained from room-temperature tensile tests carried out with the same batch of Ti6Al4V as used in the flow forming trials was used for the simulations. A constant timestep of 1 ms was used everywhere. The friction condition at mandrel and roller contact were maintained the same in all cases well. A low friction (Levanov friction factor of 0.2) and high friction (Levanov friction factor of 0.2) condition were specified at the workpiece interface with mandrel and rollers, respectively.

The temperature in the workpiece was observed to not rise beyond 50°C in experiments owing to strong coolant flow. Hence, the thermal simulation was neglected in all cases.

Results and Discussion

All three simulated cases showed reasonable agreement with roller reaction forces and final geometry observed in the experimental trials. In the experiments, it was observed that the fracture initiated on the inner surface of the workpiece in contact with the mandrel, as shown in Fig. 4(a). The trials were stopped at different instances and the fracture was identified to originate just under where roller 3 would be when it reached a depth of approx. 10 mm. Three points in the same axial plane at different depths along the thickness – Outer (surface), Mid (6 mm deep), and Inner (12 mm deep, in contact with mandrel) – corresponding to this section were identified in the simulations for further analysis, with Inner marking the location of fracture, as shown in Fig. 4(b). The same three points with exact XYZ coordinates in all three cases of simulation were tracked through the whole process, and the history of key output parameters, particularly accumulated plastic strain, triaxiality and Lode angle parameters, were traced. Furthermore, the timestamps of key events during the process, namely, Roller 1 Contact, Roller 2 Contact, Roller 3 Contact and the instance of fracture initiation with respect to the 3 identified points were recorded as shown in Fig. 4(c) and these were converted to mandrel revolutions for easy comparison.

A through-process comparison of the key output parameters from all 3 cases for the 3 identified points are presented in the following section:

Accumulated Plastic Strain.

Accumulated plastic strain or the Odquist parameter, calculated using Eq. 1 below, is an important representative scalar of the total strain path during the process and is often used in further calculations such as residual stress and fracture prediction.

$$\varepsilon^P = \int_0^t \dot{\bar{\varepsilon}}^p dt \tag{1}$$

Fig. 5 below shows a comparison of the history of accumulated plastic strain in the three cases simulated. As can be seen from Fig. 5(a), the ε^P in Case I exhibits kinks or jumps in values, which are absent in Case II and III. This can be attributed to the remeshing in Case I, wherein remeshing introduces errors in plastic strain value when remapping the calculated strain from previous time step to the newly generated mesh. Transportation of tensor values from old mesh to the new mesh poses considerable challenges and different software employ different assumptions to carry out this operation, and this introduces small errors during remapping. On repeating the operation for a few times in the case of large deformations, the errors become pronounced. This issue is not limited to QForm but is observed in other commercial FE software as well and is a challenge that warrants further in-depth study.

In addition to this, the calculated values for plastic strain in Outer and Mid points in Case I are considerably higher than those calculated in Case II and III. Given that the total reduction in thickness was 2 mm at failure, and the Mid point is 6 mm from the initial surface of the workpiece, the extremely high value of plastic strain, $\varepsilon^P = 2$, predicted for the point in Case I appears erroneous.

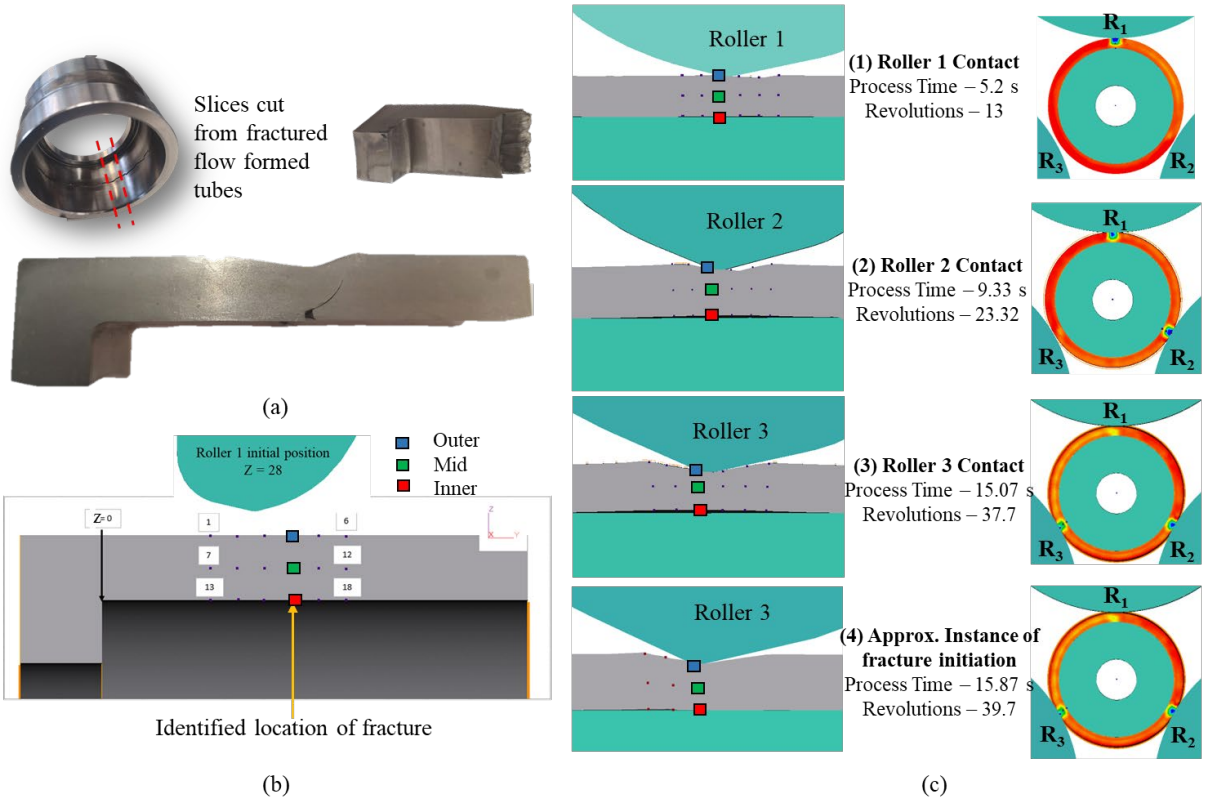

Fig. 4. Tools used for analysis of results – (a) fracture observed in experimental trials showing the location of fracture initiation, (b) points traced through the whole process in all three simulations, and (c) the timestamps of key events during the process, namely, Roller 1 Contact, Roller 2 Contact, Roller 3 Contact and instance of Fracture initiation w.r.t the points traced.

The ε^P values predicted in Case II and III appear more reliable. The difference observed in values between those calculated in Case II and Case III shows the sensitivity of the results to the mesh size used. Case III with a finer mesh can be expected to provide more accurate results in this case. Unfortunately, since the value of plastic strain cannot be directly measured but only inferred through other measurements and observations, novel calibration strategies are required to further validate the results, which are beyond the scope of this present work.

Stress-state Parameters.

Triaxiality and Lode angle parameters are important stress-state parameters that are most commonly used in fracture criteria [10, 11]. Triaxiality parameter (η), defined as the ratio of mean stress (σ_m) to equivalent or effective stress ($\bar{\sigma}$), as expressed in Eq. 2 below, is a useful parameter to represent the 3D stress-state in a point. A Triaxiality parameter of $\eta = -1/3$ represents purely uniaxial compressive stress, $\eta = 0$ represents pure shear, $\eta = 1/3$ represents purely uniaxial tensile stress and intermediate points represents a combined stress state in a point. Experimental investigation on fracture locus in Ti6Al4V show that the material is prone to fail under a tensile stress state earlier than in other conditions and $\eta >= 1/3$ are unsafe [12].

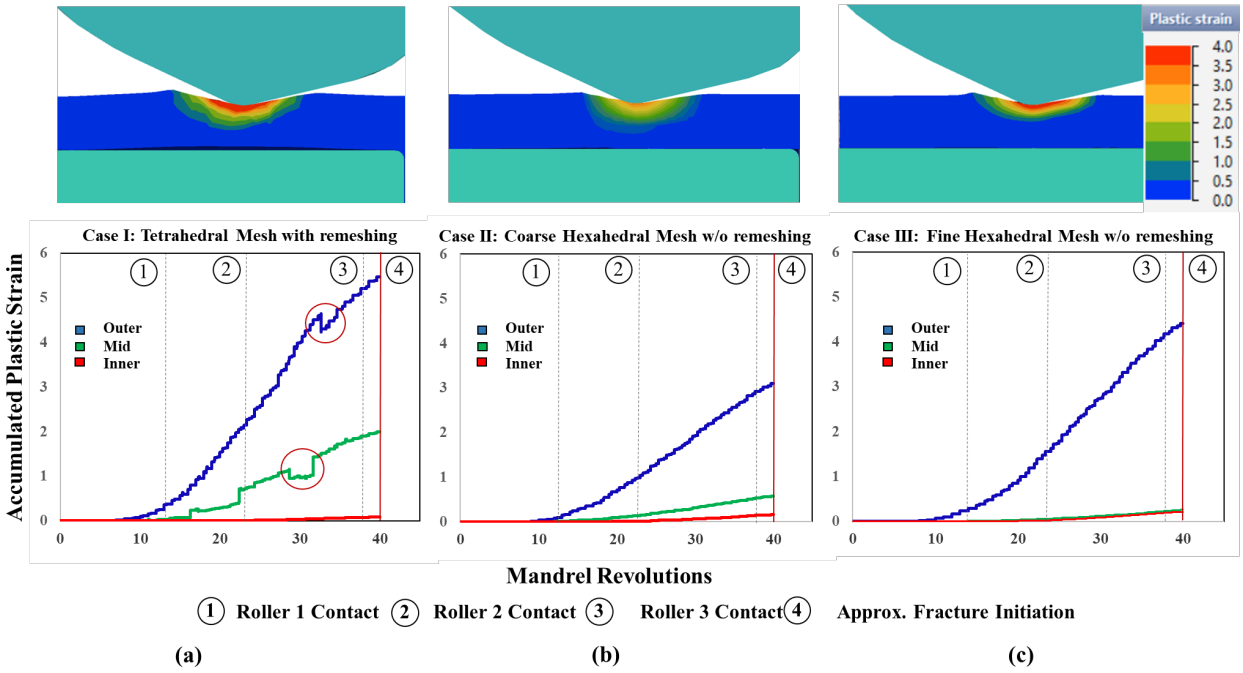

Fig. 5. Comparison of history of accumulated plastic strain in all 3 cases simulated: (a) Case I – tetrahedral mesh with remeshing, (b) Case II – Coarse hexahedral mesh, (c) Case III – fine hexahedral mesh. (Top inset: Plastic strain profile across thickness at the instance of fracture initiation in all 3 cases).

Looking at the fracture observed in flow formed Ti6Al4V tubes, the fracture appears on the inner surface where plastic strain is almost 0 and fracture surface was observed to be brittle and most probably resulted from the tensile stress state along the inner edge of the tubes directly under the rollers (refer to Fig. 6(a) and 6(b)).

$$\eta = \frac{\sigma_m}{\bar{\sigma}} \tag{2}$$

Fig. 6(c-e) shows a comparison of the history of triaxiality parameter for the same three points in all three cases studied. As can be observed, the history is considerably different in the three cases, and in Cases I and III employing a fine mesh, the deviations about the mean values are higher compared to Case II with a relatively coarser mesh. Case II and III using a Hexahedral Mesh show a trend with predominantly tensile stresses ($\eta = 1/3$) in the Inner point where fracture occurred and also in the Mid point in the initial stages closer to the contact with Roller 1. The stress state in the Mid point then transitions towards compressive stress ($\eta = -1/3$) as the reduction increases under Roller 2 and 3, which appears logical.

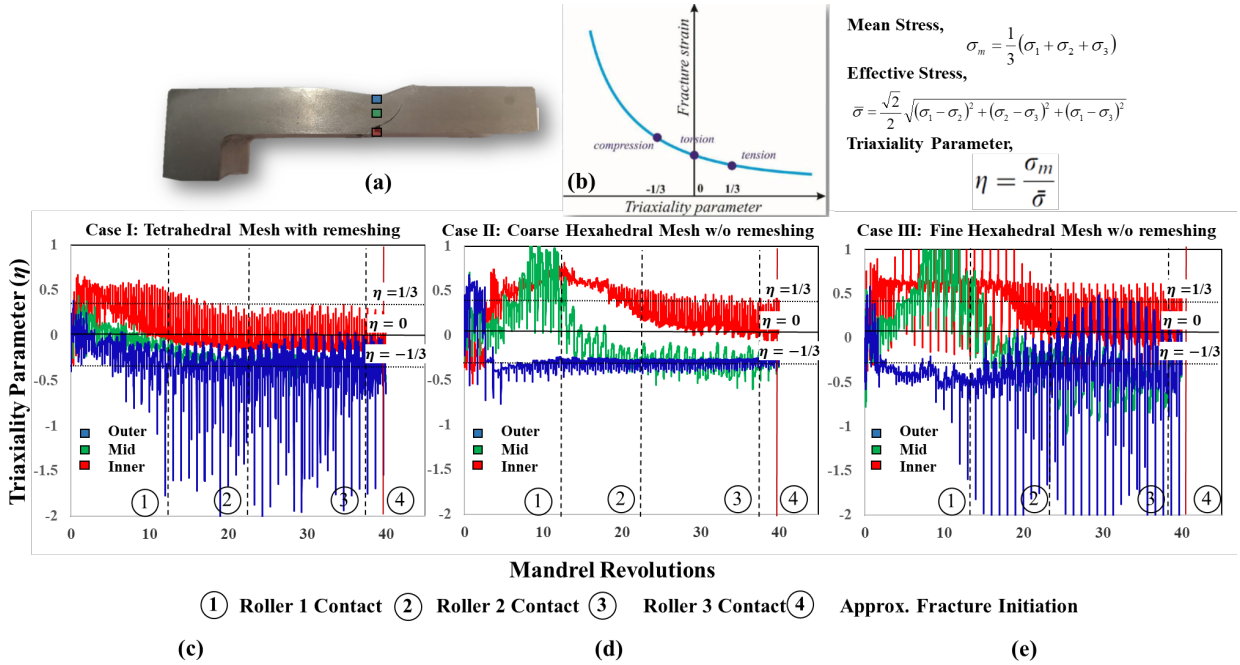

Fig. 6. Comparison of history of triaxiality parameter in all 3 cases simulated: (b) Case I – tetrahedral mesh with remeshing, (c) Case II – coarse hexahedral mesh, (d) Case III – fine hexahedral mesh. (Top inset: (a) Key: Location of points with respect to observed fracture, (b)) relationship between fracture strain and triaxiality parameter).

The duration from Roller 3 contact (Revolution 38) to the time of fracture initiation (Revolution 40) was examined further in-depth as shown in Fig. 7. The three peaks observed within a single revolution corresponds to the instant when the points are directly under the influence of the 3 rollers. As can be clearly seen in the figure, Case II and III predict tensile stresses in Inner Point, which correlates well with the main hypothesis that fracture originated in this location due to unsafe tensile stress-state prevalent at this point, while Case I does not. Case III predicts higher triaxiality and additional peaks, which warrants further investigation to be taken up in future work. Similar differences were observed in the case of Lode angle parameter as well but are not presented herein for brevity.

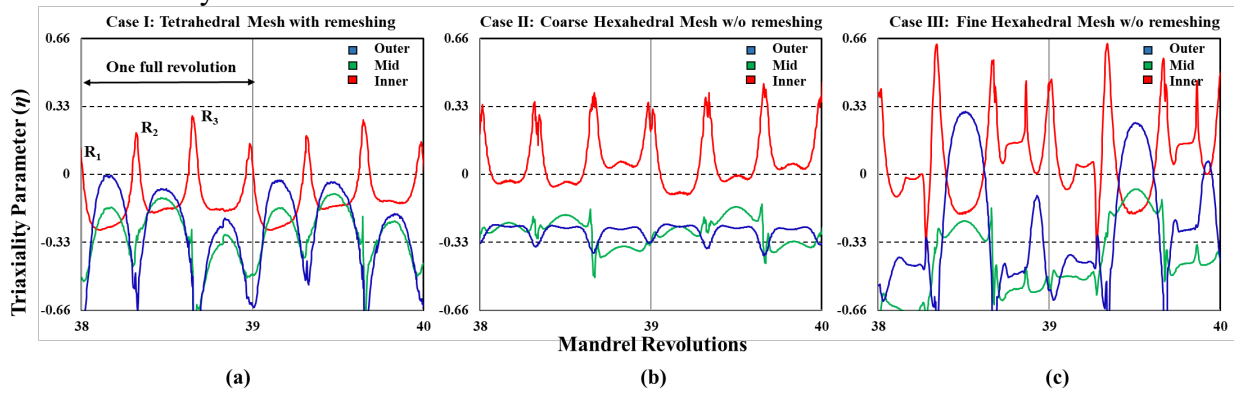

Fig. 7. In-depth comparison of history of triaxiality parameter in all 3 cases simulated in the last 2 revolutions leading up to fracture initiation.

Computation time.

The total simulation time for the three cases differed considerably and were – (i) Case I – 93 hr 24 min 48 s; (ii) Case II - 24 hr 17 min 59 s; (iii) Case III – 63 hr 49 min 13 s. It is understood that the total node count dictates the number of equations to be solved and directly influences the computation time. The total node count in the three cases simulated were - (i) Case I – 22525; (ii) Case II - 13806; (iii) Case III – 40956. As can be observed, the total simulation time in Case III was lower than that in Case I, despite having higher node count. This implies that remeshing is the chief time-consuming operation. Furthermore, in the case of hexahedral meshes, the absence of errors introduced by the remeshing operation could also lead to faster convergence of solution.

For the present case involving flow forming of Ti6Al4V tubes, hexahedral mesh appears to provide more reliable results. For cases involving large deformations and multiple passes of forming, distortion of mesh cannot be avoided without remeshing and appropriate strategies for restoring the mesh and more accurate methods for remapping the results to the restored mesh have to be investigated.

Summary

Flow forming an incremental bulk forming process with localized plastic deformations, owing to the process nature, imposes special requirements on the choice of finite element mesh and time step in simulations. Therefore, the results are highly sensitive to the mesh used. To gain a better understanding of the influence of mesh settings, 3 different cases were simulated herein - tetrahedral mesh with strain-based remeshing and two hexahedral mesh settings (relatively coarse and fine) without remeshing. A relatively short process involving a single pass flow forming of Ti6Al4V tube exhibiting fracture in the initial stages was used as the basis for model development and comparison.

- Although all cases modelled displayed comparable prediction of roller forces and output geometry, they exhibited stark differences in key output parameters, namely, accumulated plastic strain and triaxiality and Lode angle parameters that are used in critical analysis such as fracture prediction.
- For the process considered, hexahedral mesh without remeshing provided more reliable results in terms of accumulated plastic strain. Tetrahedral with remeshing provided erroneous plastic strain values in critical points in the workpiece and also introduced jumps in plastic strain history when remapping the calculated strain from previous time step to the newly generated mesh during remeshing. For short single pass flow forming, use of hexahedral mesh without remeshing is suggested as a reliable method. However, for cases involving large deformations and multiple passes of forming, distortion of mesh cannot be avoided without remeshing and more accurate methods for remapping the results during remeshing needs to be researched.
- Triaxiality and lode angle parameter from hexahedral mesh simulations without remeshing also indicate tensile stress state in the point of origin of failure, supporting the hypothesis that the fracture in question originated due to unsafe tensile stress state along the inner edge of the tube during roller penetration. The history of triaxiality and Lode angle parameters predicted using tetrahedral mesh simulation with remeshing exhibit a different trend to that observed in hexahedral mesh simulations. Before employing the results for particular problem solving such as fracture prediction, it is required to make sure that the results obtained are robust and trustable.
- Although the differences between the results are apparent and results from hexahedral mesh appear reliable when compared with experimental observation, further validation is required to improve trustworthiness of the results. Novel and intelligent validation techniques are required for this as these key output parameters are not readily measurable from experiments.

References

[1] C.C. Wong, T.A. Dean, J. Lin, A review of spinning, shear forming and flow forming processes, Int. J. Mach. Tools Manuf. 43 (2003) 1419-1435. https://doi.org/10.1016/S0890-6955(03)00172-X

[2] M. Sivanandini, S. Dhami, B. Pabla, Flow Forming Of Tubes–A Review, Int. J. Sci. Eng. Res. 3 (2012) 1-11.

[3] A. Plewiński, T. Drenger, Spinning and flow forming hard-to-deform metal alloys, Arch. Civ. Mech. Eng. 9 (2009) 101-109. https://doi.org/10.1016/s1644-9665(12)60043-0

[4] G. Ray, D. Yilmaz, M. Fonte, R.P. Keele, Metalworking: Bulk Forming, in: S. L. Semiatin (Ed.), Metalworking: Bulk Forming, ASM International, Volume 14a, 2005, pp. 516–521.

[5] Leifeld Metal Spinning AG, Spinning and Shear Forming Manual, Leifeld Metal Spinning AG, Ahlen, 2002.

[6] O.I. Bylya, T. Khismatullin, P. Blackwell, R.A. Vasin, The effect of elasto-plastic properties of materials on their formability by flow forming, J. Mater. Process. Technol. 252 (2018) 34-44. https://doi.org/10.1016/j.jmatprotec.2017.09.007

[7] O.I. Bylya, M. Ward, B. Krishnamurty, S. Tamang, R.A. Vasin, Modelling challenges for incremental bulk processes despite advances in simulation technology: Example issues and approaches, Procedia Eng. 207 (2017) 2358-2363. https://doi.org/10.1016/j.proeng.2017.10.1008

[8] M. Houillon, E. Massoni, E. Ramel, R. Logé, 3D FEM simulation of the flow forming process using lagrangian and ALE methods, AIP Conf. Proc. 908 (2007) 257-262. https://doi.org/10.1063/1.2740821

[9] H. Shinde, P. Mahajan, A.K. Singh, R. Singh, K. Narasimhan, Process modeling and optimization of the staggered backward flow forming process of maraging steel via finite element simulations, Int. J. Adv. Manuf. Technol. 87 (2016) 1851-1864. https://doi.org/10.1007/s00170-016-8559-7

[10] Y. Bao, T. Wierzbicki, On fracture locus in the equivalent strain and stress triaxiality space, Int. J. Mech. Sci. 46 (2004) 81-98. https://doi.org/10.1016/j.ijmecsci.2004.02.006

[11] G.R. Johnson, W.H. Cook, Fracture characteristics of three metals subjected to various strains, strain rates, temperatures and pressures, Eng. Fract. Mech. 21 (1985) 31-48. https://doi.org/10.1016/0013-7944(85)90052-9

[12] J.T. Hammer, Plastic deformation and ductile fracture of ti-6al-4v under various loading conditions, PhD Thesis, The Ohio State University, 2012. http://rave.ohiolink.edu/etdc/view?acc_num=osu1354700435